PV-Wind-Battery Energy System Active Power Control Using a Five Level Diode Clamped Inverter Based on SMC Controller

L.NADAM[1]|G.KIRAN[2]|M.ANJANEYELU[3]

1,2 &3 Assistant Professor, EEE department, Brilliant Institute of Engineering & Technology, Hyderabad, TS.

ABSTRACT: The power generation and stabilized quality power transmission from multiple renewable energy resources using wind, solar PV (SPV) arrays, and battery systems is covered in this manuscript. P&O strategy is used in conjunction with sliding mode control (SMC) to implement an anti-windup PI controller for active power control. The hybrid power generation (HPG) system uses a 5-level diode clamped inverter on the DC-AC conversion section for increased performance and THD improvement. It is designed for high performance with fewer switches and sensors for standalone operation. Because of its efficacy in providing extensive stability analysis and a range of operating settings for the trajectories in SMC of numerous power converters deployed within it, the HPG system is simulated using Matlab software.

KEYWORDS: SMC, THD, Diode clamped, wind.

I.INTRODUCTION: Some remote areas of the world rely solely on diesel generators (DGS) to meet their electricity requirements. This fuel source (ES) is contaminated and extremely expensive. However, given the wind and solar energy supported by the battery energy stockpiling system (BESS), a cross breed independent power generation system (HSPGS) is regarded as a promising solution for remote areas to reduce diesel-fuel dependency, limit nursery (GHS) discharges, reduce power transmission, and limit system errors [1]. Although this new innovation is feasible, it still has to be improved, especially in the plan and control to make it clear and easy to use. In the writing, ESS is suggested [2]. Multistage converters are used to link the allotted energy assets (DERs) to the point of normal coupling (PCC) in most of the suggested arrangements [3], [4], which leads to an increase in energy losses and establishment costs. In order to connect the DERs to the PCC, an AC/DC microgrid configuration is suggested in [5]. Despite the fact that the authors have succeeded in reaching their goals, this suggestion is not continuously accepted. The PCC and the sun-oriented photovoltaic exhibit (SPVA) are typically connected via single- or two-stage converters [6]. A single-stage structure is suggested in [7], and the obtained results demonstrate satisfactory execution. According to [7]–[9] and the close analysis recognized in [10], the two-stage framework exhibits a high degree of performance, especially in terms of dc voltage solidity and power quality.

With respect to productivity of SPVA, and wind turbines (WTs), numerous techniques are created in the writing to follow the maximum power point (MPP) [11], [12]. Contrasted with the current MPP following (MPPT) techniques, bother and perception (P&O) is broadly applied as a simple strategy. Shockingly, this strategy experiences the persistent swaying that happens around the MPP. What's more, it loses the following heading during unexpected changes in climate conditions. These downsides are fathomed in [13] by restricting the control utilizing dynamic limit conditions. This

arrangement is successful; notwithstanding, it requires improvement particularly in demonstrating and solidness investigation. In [14], an improved beta-P&O strategy is proposed to illuminate the downsides of the old style P&O technique. This arrangement is perplexing and its elements are moderate. Besides, it requires enormous run time since it utilizes two phases: 1) versatile scaling factor beta to get an elevated level of execution during transient reaction, and 2) zero motions P&O strategy for consistent state mistake. [15] Have introduced improvement in the exhibition of traditional P&O by utilizing delta-P&O, PIP& O, just as ZA-P&O techniques, be that as it may, with convoluted control and equipment unpredictability. In a similar setting, cross breed simple advanced sliding mode regulator (SMC) is introduced for P&O strategy in [16] to accomplish superior, particularly during climate changes, and for optimizing, the P&O-based SMC is utilized in [17]. In [18], the tip-speed proportion based SMC has been proposed for variable speed WTs. A similar methodology is applied in [19]–[21] with definite dependability examination and regulator picks up count. In every one of these examinations [9], [16]–[21], effective approval of SMC-based MPPT for SPVA and variable speed WTs, on equipment model is introduced and gotten results show agreeable execution. Be that as it may, these SMC based MPPT techniques [9], [16]–[21] are applied and approved for straightforward frameworks utilizing just a single DER with a decreased number of intensity converters, where the jabbering marvel because of high exchanging recurrence is anything but a major issue.

In a HSPGS, voltage and recurrence are directed by controlling the dc–AC interfacing inverter utilizing fitting control system, for example, versatile voltage control [22] or the new fuzzy versatile voltage regulator [23]. The introduced outcomes have indicated palatable execution anyway they require extra sensors and are unpredictable to actualize. In a similar setting, improved hang control technique is proposed in [24]–[28] for simple usage progressively. Tragically, in completely proposed control methodologies [24]–[28], the internal and external circles are utilized in traditional PI regulators and as far as possible are thought of, which isn't sufficient to forestall wrap up when the framework surpasses its physical cutoff points. In such cases, the criticism circle is broken and the framework runs as an open circle.

Power converters are plays a crucial to improve the performance of the grid connected renewable energy (RE) sources. Power generations through RE sources are gaining more attention since past decades because of its inherent properties. To obtain steady output voltages and currents from grid integrated RE sources operating power converters with a desired manner is highly needed. The performance of the total system is depending on the operation (switching pattern) of the power converters only. To produce balanced sinusoidal output voltages from the grid integrated PV systems cascaded multi-level converters are adopted. Design of various cascaded multi-level converter topologies with different PWM techniques are investigated in this project.

II. SYSTEM CONFIGURATION

The proposed HPG system with Solar PV array, wind driven variable speed PMDC generator, step-up converters, 3-ph rectifier interfacing an inverter, low-pass filter & load. For ensuring stability and effective operation of hybrid power generation system under extreme

operating conditions 3 control strategies are incorporated into the design. The fig.1 gives the brief idea of the proposed system.

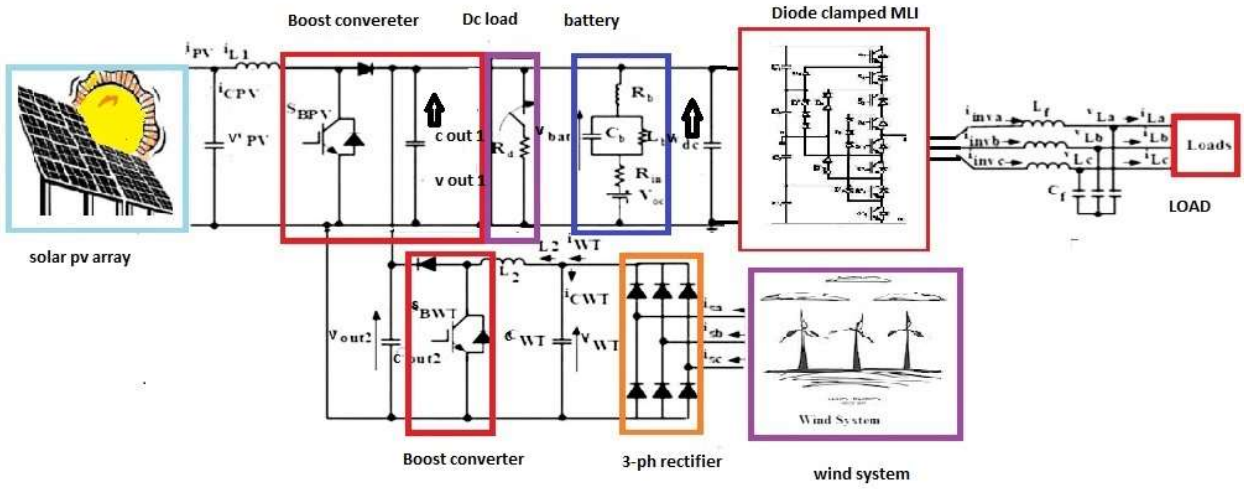

Fig.1 Proposed system

2.1Five Level Diode Clamped Inverter

The m level diode clamped inverter is designed with m-1 capacitors on the DC bus generating m phase voltage levels [22]. A single leg 5-level diode clamped multi inverter design is shown in fig. 2 with an arrangement of switches and diodes in 3 legs divvied by 4 capacitors to achieve 5 levels. The capacitor voltage Vdc is limited through clamping diodes. The table 1 lists out the various voltage levels across the capacitor and legs for deriving the 5 levels in inverter.

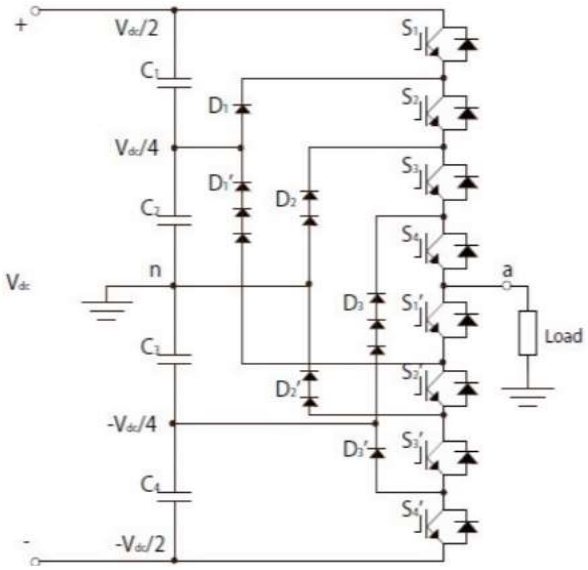

Fig.2.single leg 5-level diode clamped inverter

Table I:switching states with voltage levels in diode clamped inverter

Switching States	Output Voltages	S_1	S_2	S_3	S_4	S_1^1	S_2^1	S_3^1	S_4^1
+1	Vdc/2	1	1	1	1	0	0	0	0
+2	Vdc/4	0	1	1	1	1	0	0	0
0	0	0	0	1	1	1	1	0	0
-2	-Vdc/4	0	0	0	1	1	1	1	0
-1	-Vdc/2	0	0	0	0	1	1	1	1

The advantages of the diode clamped inverter[23-25] are as follows:

- With increased number of levels THD decreases along with the filter size.
- Faster dynamic response
- Back to back operation in the inverter is possible
- Lower switching losses.
- Active and reactive power control is possible

With advantages it exists with added limitations of high number of clamping diodes causing the power loss affecting the active power control which in turn complicates the systems control.

The diode clamped five level multi inverters is widely used in medium and high voltage applications, as it has many advantages with least complex framework in contrast to higher level (7 or 9) inverters.

2.2 Sinusoidal PWM Technique:

In this technique[26] sinusoidal modulating voltage of the expected output frequency f_o is contrasted with a higher frequency triangular waveform or a saw tooth carrier waveform to create the pulsating signals for the inverter. The amplitude decides RMS estimation of the output voltage. The subsequent exchanging pulses have widths around corresponding to the sine of the rakish position at the focal point of the pulses. The widths of these pulses are likewise corresponding to the sufficiency of the modulating signal comparative with the amplitude of the carrier waves.

This technique has been integrated with the diode clamped multi inverter for the better performance in switching of the diodes while yielding the regulated output voltage with desired higher efficiency in pv-wind-battery energy system with SMC controller based five level diode clamped inverter.

3.MODELING AND CONTROL STRATEGIES

This section deals with the development of the proposed system with solar PV system, wind system, power converters with integrated control strategies for stability and reliability analysis.

3.1 Modeling and Control Design for SPVA

From figure.1 modeling of boost converter with solar PV array is as follows:

$$L_1(\partial i_{L1}/\partial t) = \vartheta_{PV} \quad (1)$$

$$C_{01}(\partial \vartheta_{01}/\partial t) = - \vartheta_{01}/R \quad (2)$$

$$I_{CPV}=C_{PV}(\partial \vartheta_{CPV}/\partial t) = i_{PV}-i_{L1} \quad (3)$$

But with switchS_{BPV}= 0 (OFF state) we get

$$L_1(\partial i_{L1}/\partial t) = - \vartheta_{01} \quad (4)$$

$$C_{01}(\partial \vartheta_{01}/\partial t) = i_{L1} - (\vartheta_{01}/R) \quad (5)$$

L_1=inductance R-resistive branch C_{PV}=input capacitance C_0=output capacitance

$\vartheta_{CPV\&}\vartheta_{01}$=input and output capacitive voltages

Simplifying the equations from (1-5) we get (6-7) as boost voltage equations which are

$$(\partial i_{L1}/\partial t) = (\vartheta_{PV}/L_1) - (1-d_1)(\vartheta_{01}/L_1) \quad (6)$$

$$(\partial \vartheta_{01}/\partial t) = (1/C_{01})[(i_{L1}(1-d_1)) - (\vartheta_{01}/R)] \quad (7)$$

$$(\partial i_{PV}/\partial t) = \{(\vartheta_{PV}/L_1) - (1-d_1)(\vartheta_{01}/L_1)\} + \{C_{PV}(\partial^2 \vartheta_{PV}/\partial^2 t)\} \quad (8)$$

1st Term 2nd Term

d_1 =desired control

The variation of ϑ_{pv}=0. Hence the equation (8) is re written as

$$(\partial i_{PV}/\partial t) = (\vartheta_{PV}/L_1) - (1-d_1)(\vartheta_{01}/L_1) \quad (9)$$

3.1.1Boost converter-1 control strategy:

The below figure indicates the improved form of P&O approach with specified saturation limits for achieving high rate of efficiency from solar pv modules even under partial shading conditions.

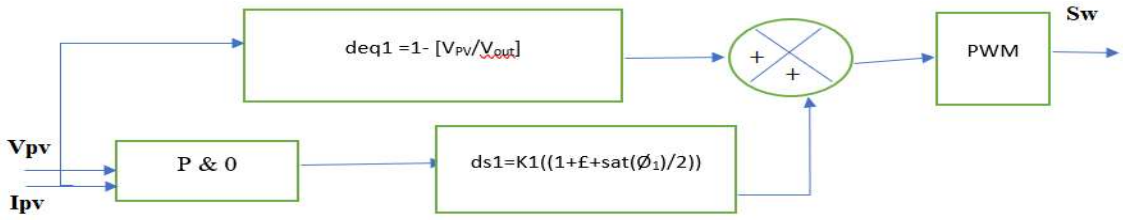

Fig.3. Improved P&O SMC for Solar PV

Selecting a Sliding surface:

To derive the maximum MPPT[27] out of system sliding surface selection designing is based on

$$\sigma_1 = (\partial P_{PV}/\partial i_{PV}) = 0 \quad (10)$$

P_{PV}=generated Photo Voltaic power which is

$$P_{PV} = \vartheta_{PV} i_{PV} \quad (11)$$

Substituting (11) in (10) obtains,

$$\sigma_1 = (\partial P_{PV}/\partial i_{PV}) = \partial (\vartheta_{PV} i_{PV})/ \partial i_{PV} \quad (12)$$

which in turn is derived as

$$\sigma_1 = \vartheta_{PV} + i_{mPV}(\partial \vartheta_{PV}/\partial i_{mPV}) \quad (13)$$

i_{mPV} = output PV current from the classical P&O

3.2 Model of the Equivalent Control:

3.2.1 The control is derived by fixing the derivative of equation (13) to zero.

The structure of the control (d1) is communicated as

$$d_1 = d_{eq1} + d_{s1} \quad (14)$$

$$d_{s1} = k_1 ((1 + \varepsilon + sat (\sigma_1, \Phi_1))/2) \quad (15)$$

including

$$sat(\sigma_1, \Phi_1) \begin{cases} 1 & \sigma_1 \succ \Phi_1 \\ \sigma_1/\Phi_1 & |\sigma_1| \leq \Phi_1 \\ -1 & \sigma_1 \prec -\Phi_1 \end{cases} \quad (16)$$

where

k1 = positive control gain

d_{eq1}= equivalent control

Φ1 = sliding layer, which is between 0.5 and −0.5

$$\frac{\partial \sigma 1}{\partial t} = (\partial \sigma_1/\partial i_{mPV}) (\partial i_{mPV}/\partial t)$$

$$= (\partial \sigma_1/\partial i_{mPV})[(\frac{\vartheta PV}{L1}) - (1-d_1) (\frac{\vartheta 01}{L1})] \quad (17)$$

The nontrivial form of solution on (17) is as follows:

$$\vartheta_{PV} - (1-d_1) \vartheta_{01} = 0 \quad (18)$$

and the equivalent control is obtained as

$$d_{eq1} = 1- (\vartheta_{PV}/ \vartheta_{01}) \quad (19)$$

3.2.2 System Stability Analysis:

The Lyapunov function used for verifying the system stability is

$$V_1 = (1/2) \sigma_1^2 \quad (20)$$

The framework is comprehensively steady if the subordinate of (20) is negative as

$$(\partial V_1/\partial t) = \sigma_1 (\partial \sigma_1/\partial t) < 0 \quad (21)$$

Altering (13) and (17) into (21) gives (22), which consists of terms as

$$\{\vartheta_{PV} + i_{mPV} (\partial \vartheta_{PV} /\partial i_{mPV})\}$$
$$x\{2(\partial \vartheta_{PV} /\partial i_{mPV}) + i_{mPV} (\partial^2 \vartheta_{PV} /\partial^2 i_{mP\,V})\}\ x\{((\vartheta_{PV}/L_1) - (1-d_1) (\vartheta_{01}/ L_1)\}<0 \quad (22)$$

where $\vartheta_{PV=}$ PV output voltage and denoted as

$$\vartheta_{PV} = (K_b\ T\ A / q) \ln ((i_{ph} + i_D – i_{L1})/ i_D) \quad (23)$$

k_b= Boltzmann's constant T= cell temperature

A= ideality factor Q= charge of an electron

I_{ph}= light generated current i_D,i_L= PV currents

It is seen in (22) that term1 and term contain the first and the second subordinates of output voltages of PV (V_{PV}). To confirm the indication of (21), we supplant the first and second subsidiaries of ϑ_{pv} which are derived as (24) and (25) into (22) &are supplanted as follows.

$$(\partial \vartheta_{PV}/\partial i_{L1}) = -\{(K_b\ T\ A / q)\} x \{(i_D/ (i_{ph} + i_D – i_{L1})\} \quad (24)$$

Term 1 Term 2

$$(\partial^2 \vartheta_{PV}/\partial^2 i_{L1}) = -\ \{K_b\ T\ A / q)\}\{i_D/ (i_{ph} + i_D – i_{L1})^2\} \quad (25)$$

To confirm the soundness of the condition characterized in equation (21), & the terms in equation (22) must be resolved. Light gen current (i_{ph}) in 2nd term of equation (23) is more noteworthy than the immersion current (i_D) which is more than the inductor current (i_{L1}). Be that as it may, 2nd term is positive and smaller. The indication of the 1st term of equation (22) is certain and is determined utilizing actual saturation limits of solar PV denoted as:

Table II: SYSTEM PARAMETERS

Element	Specifications
PV side	Irr = 5.98x10^{-8} A, K_i = 0.0024A, Eg = 1.12V Cout = 1000 µF, L_1 = 1.5mH
WT side	Rs =0.808 ohms, Ls =5.44mh, Vs =208V, L_{wT} =1.5mH, J=0.01859kg
DC bus	V_{dc} = 105V, 12V lead acid batteries
AC side	f=60Hz, V_{LL} =50V, L_f =5mH, C_f = 40µF

$$\{(\vartheta_{01}/ L_1\}\ k_1\ \{(1 + \varepsilon + sat\ (\sigma_1, \Phi_1))/2)\} > 0 \quad (26)$$

1st term 2nd term

The above term is always positive in the mathematical analysis.

3.3. Design and Control of WT:

The design of PMDC generator and its specific parameter are described here

3.3.1 Mathematical Model of PMDC generator:

The balance equation for PMDC generator is expressed as

$$[\vartheta_{spqr}] = R_s[i_{spqr}] + (L_s - M)\,[di_{spqr}/\partial t] + [e_{pqr}] \quad (27)$$

The produced electromagnetic torque (T_e) is

$$T_e = (1/\omega_r)\,(e_a i_{WPa} + e_b i_{WPb} + e_c i_{WPc}) \quad (28)$$

$$\omega_r = (2/P)\,\omega_e \quad (29)$$

Mechanical torque (T_m) is

$$T_m = T_e + J\,(d\omega_r/dt) + B\omega_r \quad (30)$$

3.3.3Control Strategy for Boost Converter-2:

The control scheme of improved P&O MPPT based PV array is shown in below fig.3

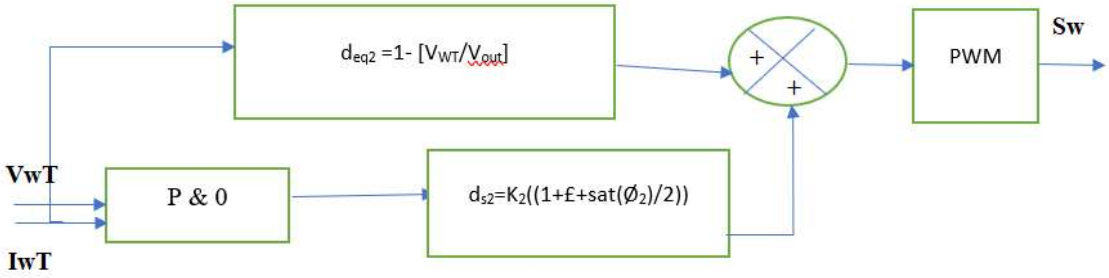

Fig.4. Improved P&O

IV. SIMULATION RESULTS

4.1. Performance of PV-Wind Battery Energy system under steady state:

In this case a constant 5kW load is considered on PV-Wind-Battery energy system, balanced 105Volts appeared across at DC link capacitor. Steady state load voltage and current is obtained with proposed control scheme. The obtained simulation results of DC link voltage, load voltage, load current and system frequency is illustrated in fig7a to fig7d respectively.

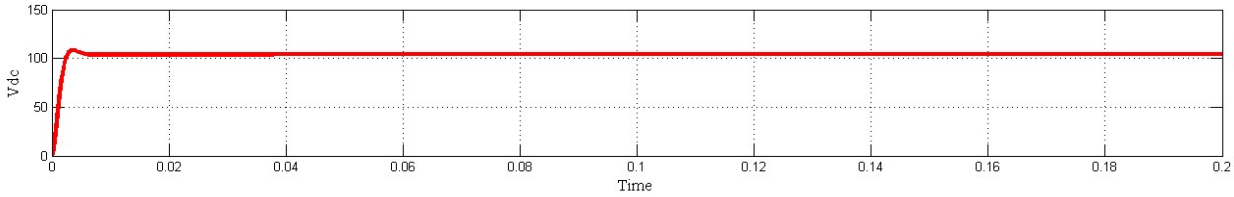

Fig.7a. DC link Voltage

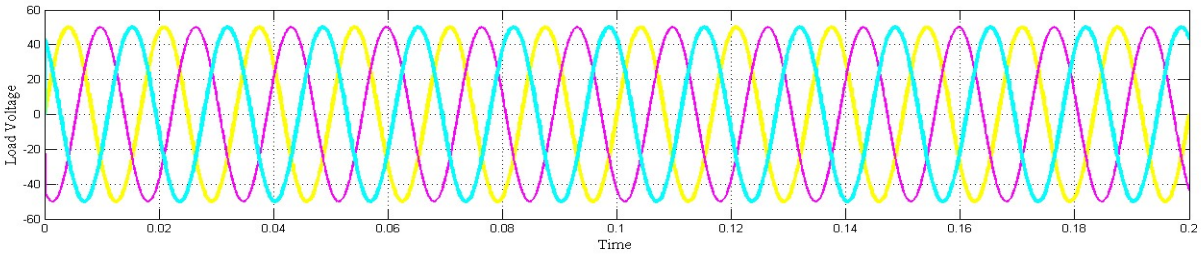

Fig.7b. Load Voltage

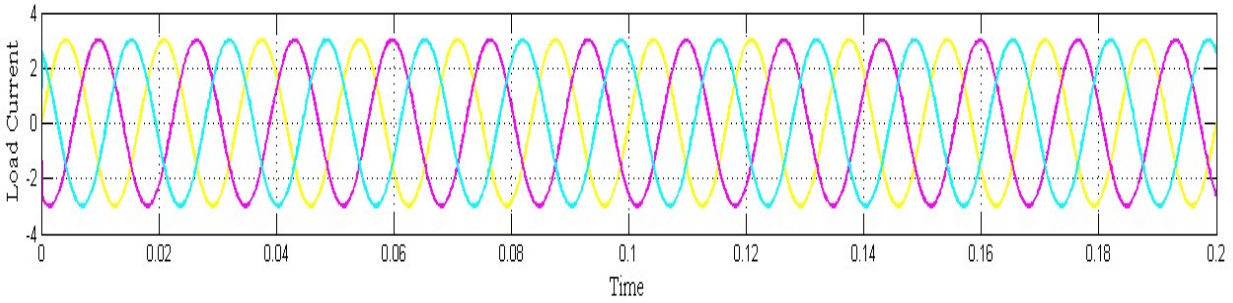

Fig.7c.Load Current

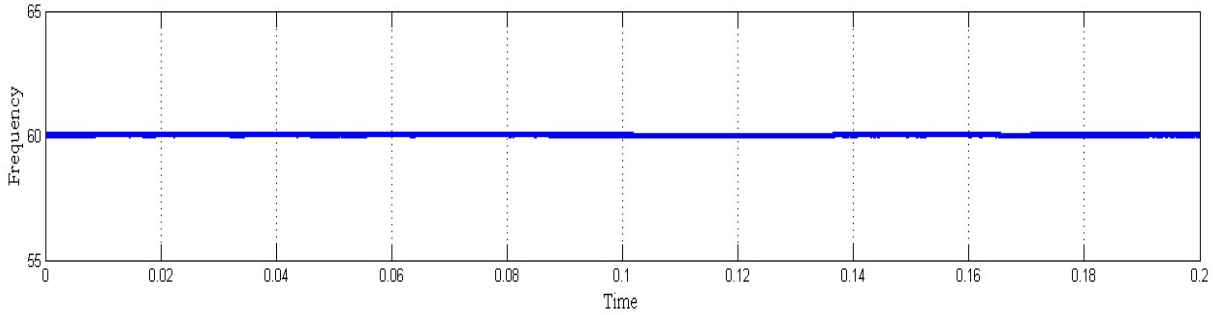

Fig.7d. System Frequency

4.2. Performance of PV-Wind Battery Energy system with sudden varying load:

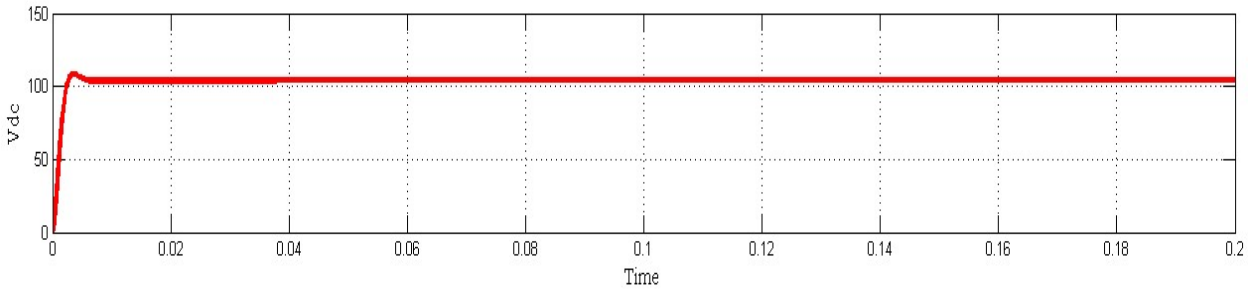

Fig.8a. DC link Voltage

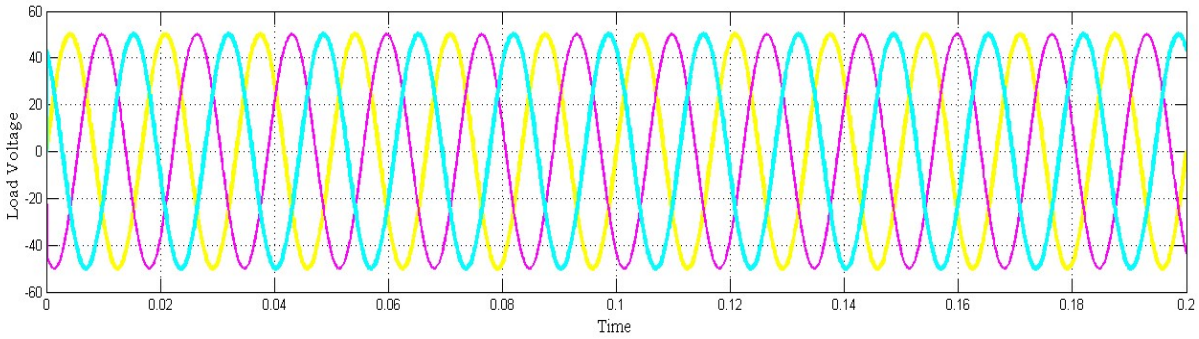

Fig.8b. Load Voltage

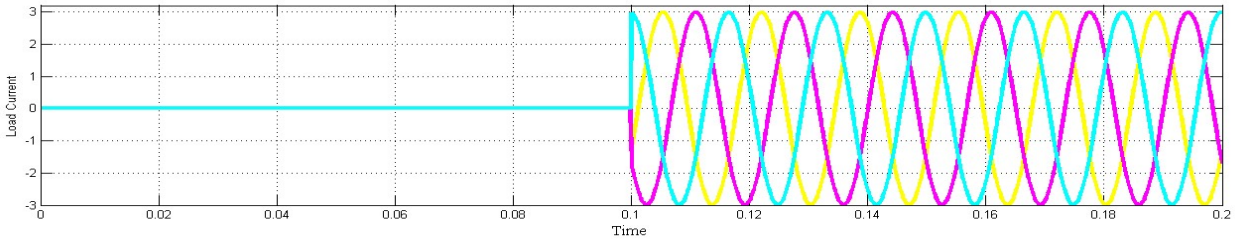

Fig.8c. load current

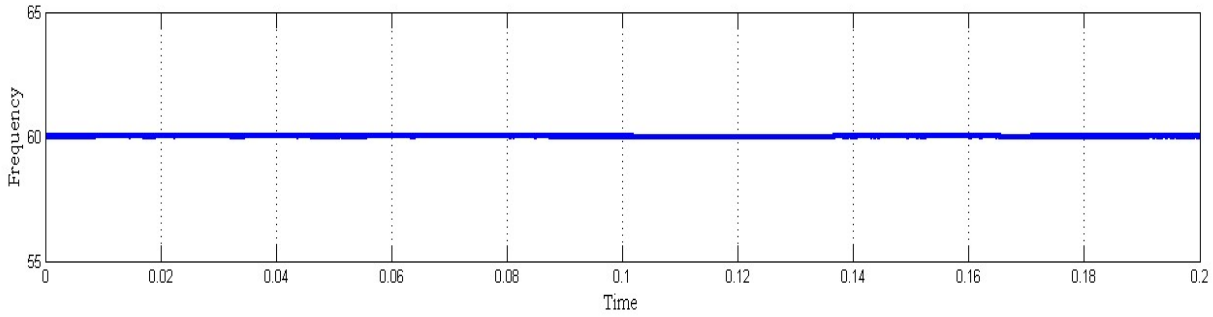

Fig.8d. system frequency

4.3. Performance of PV-Wind Battery Energy system with unbalance linear load:

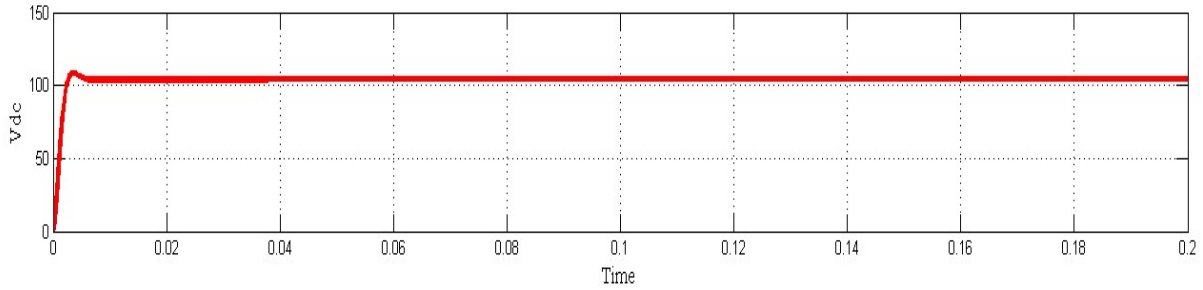

Fig.9a DC link voltage

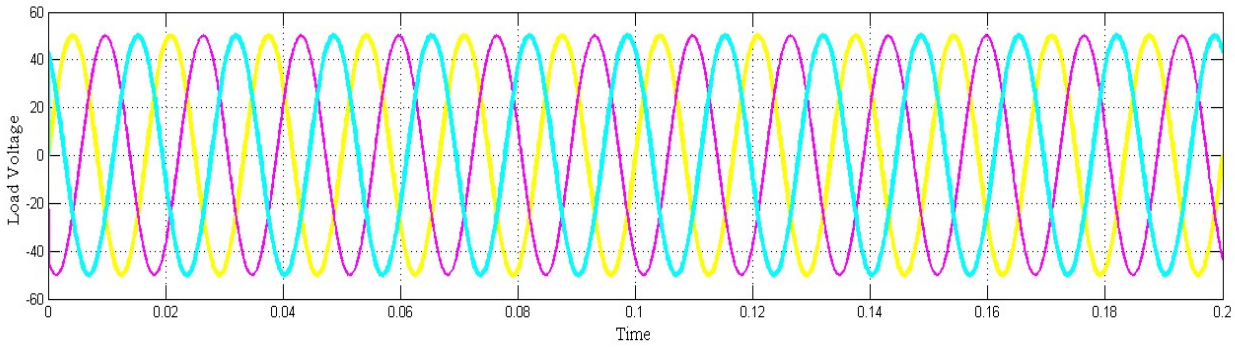

Fig.9b load voltage

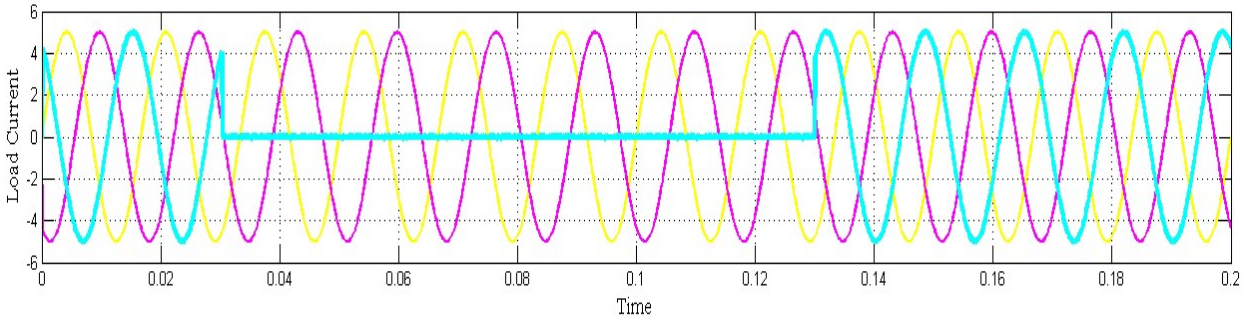

Fig.9c load current

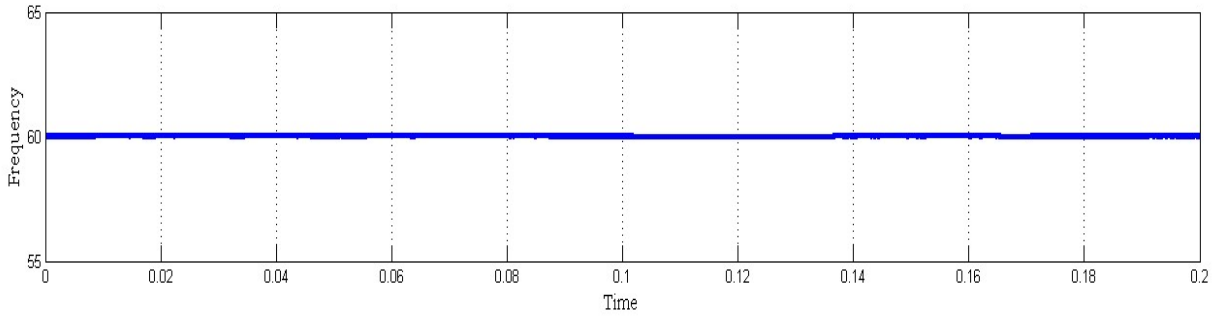

Fig.9d. system frequency

V. CONCLUSION

In the paper, a P&O-based HPG system with an antiwind PI controller and built-in SMC is successfully designed and simulated, meeting the predetermined theoretical analysis. In order to achieve consistent and desirable sinusoidal voltages without clipping off during saturation and overshoots, the proposed model is made to improve control and stability of MPPT of solar PV systems and wind systems integrated with anti-wind PI controller. When compared to earlier studies, the simulations have demonstrated improved outcomes with dependable performance and reduced THD even under erratic loads and weather.

REFERENCES

[1] Sudhakar A.V.V, Vodela Naga Santhosh and Md. Mujahid Irfan, "Detection Of Partial Shading Condition And Extraction Of Maximum Power From Shaded PV Array With Fuzzy Controller" in IJMPERD ISSN(P): 2249–6890; ISSN(E): 2249–8001 Vol. 10, Issue 3, pp.8597–8606 Jun 2020.

[2] H.G. Kim, D.C. Lee, J.K. Seok and G.M. Lee, "Stand-alone wind power generation system using vector-controlled cage-type induction generators," in Proc. of Inter. Conference on Electrical Machines and systems, vol.1, pp.289-292, Nov.2003.

[3] P. Satish Kumar, R.P.S. Chandrasena and K. Victor Sam Moses Babu, Design and Implementation of Wind Turbine Emulator using FPGA for Stand Alone Applications, International Journal of Ambient Energy, Taylor and Francis Publications, March 2020.

[4] S. K. Kollimalla, M. K. Mishra and N. L. Narasamma, "Design and Analysis of Novel Control Strategy for Battery and Supercapacitor Storage System," in *IEEE Transactions on Sustainable Energy*, vol. 5, no. 4, pp. 1137-1144, Oct. 2014.

[5] L. Minchala-Avila, L. Garza-Castanon, Y. Zhang, and H. Ferrer, "Optimal energy management for stable operation of an islanded microgrid," IEEE Trans. Ind. Inf., vol. 12, pp. 1361–1370, Aug. 2016.

[6] P. Satish Kumar, R. P. S. Chandrasena, V. Ramu, G. N. Srinivas, K. Victor Sam Moses Babu, "Energy Management System for Small Scale Hybrid Wind Solar Battery Based Microgrid" IEEE Access Journal, Vol. 8, pp. 8336 – 8345, Jan. 2020.

[7] M. A. G. d. Brito, L. Galotto, L. P. Sampaio, G. D. A. E. Melo, and C. A. Canesin, "Evaluation of the main MPPT techniques for photovoltaic applications," IEEE Trans. Ind. Electron., vol. 60, no. 3, pp. 56–67, Mar. 2013.

[8] K. H. Kim, T. L. Van, D. C. Lee, S. H. Song, and E. H. Kim, "Maximum output power tracking control in variable-speed wind turbine systems considering rotor inertial power," IEEE Trans. Ind. Electron., vol. 60, no. 8, pp. 3207–3217, Aug. 2013

[9] Ohnuki et al., "Control of a Three-Phase PWM Rectifier Using Estimated AC-Side and DC-Side Voltages," IBEE Transactions on Power Electronics, vol. 14, No. 2, (Mar. 1999). pp. 222-226.

[10] Wang Y, Han F, Yang L, Xu R, Liu R. A three-port bidirectional multi-element resonant converter with decoupled power flow management for hybrid energy storage systems. IEEE Access 2018. 1-1.